Water-Based Route to Colloidal Mn-Doped ZnSe and Core/Shell ZnSe/ZnS Quantum Dots

Abdelhay Aboulaich, Malgorzata Geszke, Lavinia Balan, Jaafar Ghanbaja, Ghouti Medjahdi, Raphaël Schneider

HAL Id: hal-00784880
https://hal.science/hal-00784880

Submitted on 19 Feb 2013

Water-based route to colloidal Mn-doped ZnSe and core/shell ZnSe/ZnS quantum dots

*Abdelhay Aboulaich,[†] Malgorzata Geszke,[†,‡] Lavinia Balan,[§] Jaafar Ghanbaja,[#] Ghouti Medjahdi,[ξ] Raphaël Schneider[†,]**

Laboratoire Réactions et Génie des Procédés (LRGP), UPR 3349, Nancy-University, CNRS, 1 rue Grandville, 54001 Nancy Cedex, France

Department of Pharmaceutical Technology, Poznan University of Medical Sciences, Grunwaldzka 6, 60-780 Poznan, Poland

Institut de Science des Matériaux de Mulhouse (IS2M), LRC 7228, 15 rue Jean Starcky, 68093 Mulhouse, France

SCMEM, Nancy-University, BP 70239, 54506 Vandoeuvre-lès-Nancy Cedex, France

IJL, Nancy-University, BP 70239, 54506 Vandoeuvre-lès-Nancy Cedex, France

raphael.schneider@ensic.inpl-nancy.fr

* To whom correspondence should be addressed. Phone: +33 3 83 17 50 53. E-mail: raphael.schneider@ensic.inpl-nancy.fr

† LRGP, Nancy-University

‡ Poznan University of Medical Sciences

§ IS2M, Université de Haute Alsace

SCMEM, Nancy-University IJL, Nancy-University

ξ IJL, Nancy-University

Relatively monodisperse and highly luminescent Mn^{2+}-doped zinc blende ZnSe nanocrystals were synthesized in aqueous solution at 100°C using the nucleation-doping strategy. The effects of the experimental conditions and of the ligand on the synthesis of nanocrystals were investigated systematically. It was found that there were significant effects of molar ratio of precursors and heating time on the optical properties of ZnSe:Mn nanocrystals. Using 3-mercaptopropionic acid as capping ligand afforded 3.1 nm wide ZnSe:Mn QDs with very low surface defect density and which exhibited the Mn^{2+}-related orange luminescence. The post-preparative introduction of a ZnS shell at the surface of the Mn^{2+}-doped ZnSe QDs improved their photoluminescence properties, resulting in stronger emission. A 2.5-fold increase in photoluminescence quantum yield (from 3.5 to 9%) and of Mn^{2+} ion emission lifetime (from 0.62 to 1.39 ms) have been observed after surface passivation. The size and the structure of these QDs were also corroborated by using transmission electron microscopy, energy dispersive spectroscopy and X-ray powder diffraction.

1. Introduction

Semiconductor nanocrystals or quantum dots (QDs) have become one of the most attractive areas of current research because of their tremendous potential applications in photonic devices, biological detection and labelling and imaging.[1-6] The wide interest in QDs arises from their unique optical and electrical properties, including broad absorption and narrow emission spectra, large extinction coefficients, resistance to photobleaching, long fluorescence lifetime, and size-tunable emission.[7-9] Moreover, QDs with different emission colors can be simultaneously excited with a single light source, with minimal spectral overlap, thus providing significant advantages for multiplexed detection of molecular targets.[10-12]

During the last ten years, cadmium-based QDs, and especially core/shell CdSe/ZnS, have been the workhorse of the QD emitters. Because of the ultimate elimination of highly toxic class A elements like Cd, Hg and Pb, numerous researches are currently conducted to develop QDs without any heavy metal. Transition element-doped nanocrystals (d-dots) can be an alternative to Cd-based ones for numerous applications.[13-14] Over the various non-cadmium II-VI semiconductors that constitute hosts for dopants, zinc selenide ZnSe with a room temperature bulk band gap of 2.80 eV (442 nm) is especially interesting because it is widely used for various applications like light-emitting diodes (LEDs), photovoltaic solar cells, photocatalysts, and biological sensors.[15-18] In d-dots, the dopants lead to phenomena not found in the bulk state because their electronic states are confined in a very small volume. Mn^{2+} is one of the most common dopant for many II-VI semiconductors because (i) its location inside the crystal lattice of the host material can be confirmed by electron paramagnetic resonance (EPR), and (ii) it exhibits a typical photoluminescence from the Mn^{2+} $^4T_1 \rightarrow {}^6A_1$ transition centered at ca. 595 nm.[19]

Over the last ten years, a few groups have reported the synthesis of ZnSe[20-25] and of the related Mn-doped ZnSe nanocrystals[26-33] via organometallic synthesis. This approach generally utilizes pyrolysis of organometallic complexes in coordinating solvents such as tri-*n*-octylphosphine (TOP) or tri-*n*-octylphosphine oxide (TOPO). The exchange of the hydrophobic TOP or TOPO ligands with

3

hydrophilic ligands, such as thioacids, and subsequent transfer of QDs from oil to aqueous solution can significantly reduce the photoluminescence quantum yield (PL QY) of the nanocrystals.[2] Direct synthesis of thiol-capped QDs in water is a promising alternative route to organometallic reactions and offers the following advantages: (1) it uses less toxic reagents, (2) it is cheaper and simpler, (3) it uses lower reaction temperatures (100°C) to obtain QDs with comparable PL QY and size-tunable fluorescence, (4) the surface functionalization with water-soluble ligands occurs during the synthesis, and (5) the QDs obtained have a small diameter, which is suitable for biological applications. Recent studies have demonstrated that good quality ZnSe QDs can be prepared in water either under hydrothermal conditions[34-39] or under microwave irradiation[40] by reaction of a Zn(+2) salt with NaHSe, generally in the presence of a thioalkyl acid stabilizer. Using a mixture of the dopant and of the host precursor during the nucleation step (also called nucleation-doping strategy), Wang *et al.* succeeded recently in the preparation of Mn^{2+}-doped ZnSe QDs with a PL QY of 2.4%, which represents the first direct synthesis of fluorescent Mn^{2+}-doped ZnSe QDs in aqueous solution.[41]

In the present study, we report an alternative aqueous route to prepare ZnSe:Mn QDs stabilized by 3-mercaptopropionic acid (MPA). The trap state emission at 480 nm of the d-dots obtained was found to be very weak and could completely be suppressed by passivating the Mn-doped ZnSe core material with the wider band gap shell material ZnS. Using this strategy, MPA-capped core/shell ZnSe:Mn/ZnS nanocrystals with PL QYs up to 9% in water at neutral pH could be readily prepared.

2. Experimental Section

2.1. Reagents and Materials. Zinc sulfate heptahydrate ($ZnSO_4 \cdot 7H_2O$, 99.99%), zinc acetate dihydrate ($Zn(OAc)_2 \cdot 2H_2O$, 98+%), manganese acetate tetrahydrate ($Mn(OAc)_2 \cdot 4H_2O$, 99%), mercaptopropionic acid (MPA, 99%), selenium powder (99.5%, 100 mesh), sodium borohydride ($NaBH_4$, 98%), and ethanol (HPLC grade) were used as received without additional purification. All solutions were prepared using Milli-Q water (18.2 $M\Omega.cm^{-1}$, Millipore) as the solvent.

4

2.2. Synthesis of ZnSe:Mn QDs. The preparation of NaHSe was performed according to Klayman *et al.*[42] with some modifications. Under an argon atmosphere, 76 mg (2.009 mmol) of $NaBH_4$ was added to a small flask cooled with ice containing 1 mL of ultrapure water. 79 mg (1.004 mmol) of selenium powder was then added and a small outlet was connected to the flask to discharge the hydrogen pressure generated by the reduction of Se into NaHSe. After 3 h at 4°C, the black selenium powder disappeared and a white NaHSe solution was obtained. The solution was diluted with 20 mL of argon-saturated water and the concentration of the final NaHSe solution was 0.05 M.

Typical procedure for the preparation of MPA-capped ZnSe:Mn QDs: Solutions of 0.1 M $ZnSO_4$. $7H_2O$ (5 mL), 0.01 M $Mn(OAc)_2$. $4H_2O$ (2 mL) for a Mn^{2+} doping of 4% relative to Zn^{2+} and 0.5 M MPA (20 mL) were mixed and the pH of the mixture was adjusted to 10.3 by dropwise addition of a 2 M NaOH solution. The solution was placed in a three-necked flask fitted with a septum and valves, and further stirred under argon for 1 h. 9 mL of a freshly prepared NaHSe solution (0.05 M) were then injected through a syringe into the mixture at room temperature. The molar ratio $Zn^{2+}/Se^{2-}/MPA$ in the solution was 1/0.9/20. The growth of the MPA-capped ZnSe:Mn nanocrystals proceeded on refluxing at 100°C for 24 h under argon flow with a condenser attached. After cooling to room temperature, the MPA-capped ZnSe:Mn nanocrystals were precipitated by ethanol, the precipitate was centrifuged, washed 3 times with ethanol, and then dried in vacuum (30 mmHg, 2 h, rt).

Thioglycolic acid (TGA), 6-mercaptohexanoic acid (MHA), mercaptosuccinic acid (MSA), and cysteine(Cys)-capped ZnSe:Mn QDs were prepared at pH = 10.3 using a molar ratio of $Zn^{2+}/Se^{2-}/ligand$ of 1/0.9/20, similarly to MPA-capped QDs.

2.3. Synthesis of MPA-capped ZnSe:Mn/ZnS core/shell nanocrystals. For the ZnS shell growth, 10 mL of 0.2 M $Zn(OAc)_2$. $2H_2O$ solution and 0.7 mL of MPA were mixed together and the solution was diluted to 88 mL with water. The pH was adjusted to 10.3 with 4 M NaOH and the solution was saturated with argon by bubbling for 1h. The ZnSe:Mn core solution was prepared by dispersing 20 mg of ZnSe:Mn QDs in 130 mL of water, transferred into a three-necked flask fitted with a septum and valves and purged by argon bubbling for 1h. Then, 20 mL of the Zn^{2+}-MPA complex were added

dropwise to the ZnSe:Mn solution and the mixture was heated at 100°C for 10 h. After cooling to room temperature, the reaction mixture was concentrated down to approximately 15 mL, nanocrystals were precipitated with ethanol and dried in vacuum at room temperature for 12 h before measurements.

2.4. Instruments. Transmission electron microscopy (TEM) images were taken by placing a drop of the particles in water onto a carbon film-supported copper grid. Samples were studied using a Philips CM20 instrument operating at 200 kV equipped with Energy dispersive X-ray Spectrometer (EDX). The X-ray powder diffraction (XRD) diagrams of all samples were measured using Panalytical X'Pert Pro MPD diffractometer using Cu Kα radiation ($\lambda = 1.5405$ Å). Absorption spectra were recorded on a Perkin-Elmer (Lambda 2) UV-Visible spectrophotometer. Fluorescence spectra were recorded on a fluorolog-3 spectrofluorimeter F222 (Jobin Yvon) using a 450 W xenon lamp. The QY values were determined from the following equation:

$$QY(sample) = (F_{sample}/F_{ref})(A_{ref}/A_{sample})(n_{sample}^2/n_{ref}^2)QY_{(ref)}$$

where F, A and n are the measured fluorescence (area under the emission peak), absorbance at the excitation wavelength and refractive index of the solvent respectively. PL spectra were spectrally corrected and quantum yields were determined relative to Rhodamine 6G (QY = 94%).[43] The fluorescence lifetimes were measured by a FluoroMax-4 spectrofluorometer (Jobin Yvon) using a NanoLED emitting at 372 nm as an excitation source with a nanoled controller module, Fluorohub from IBH, operating at 1 MHz. The detection was based on an R928P type photomultiplier from Hamamatsu. Fourier transform infrared spectroscopy (FT-IR) was performed using a Brucker Vector 22 spectrometer. Dynamic light scattering (DLS) was performed at room temperature using a Malvern zetasizer HsA instrument with a He-Ne laser ($4 \cdot 10^{-3}$ W) at a wavelength of 633 nm. The QDs aqueous solutions were filtered through Millipore membranes (0.2 μm pore size). The data were analyzed by the CONTIN method to obtain the hydrodynamic diameter (d_H) and the size distribution in each aqueous dispersion of nanoparticles.

3. Results and discussion

A series of ZnSe:Mn QDs were synthesized in aqueous solution containing thioalkylacids (thioglycolic acid TGA, 3-mercaptopropionic acid MPA, 6-thiohexanoic acid MHA, mercaptosuccinic acid MSA or cysteine Cys). Thioalkyl acids contain two functional groups possessing lone pair electrons that might influence the nucleation, the growth and the stabilization of ZnSe:Mn QDs and hence affect their physical and optical properties. Since the synthesis of the d-dots is conducted at basic pH, the negative charges of thioalkyl acids will also impose a kinetic barrier for the growth due to Coulombic repulsions between the ligand shells of neighboring QDs and thus favour stable and small nanocrystals.

3.1. Preparation of Thioalkyl Acid-capped ZnSe:Mn Nanocrystals. We first studied the synthesis and the optical properties of 3-mercaptopropionic acid-capped ZnSe nanocrystals.

Influence of the Zn/Se ratio and of the Zn^{2+} concentration. Initial experiments performed with 4 % doping in Mn^{2+} and a 2.7 mM $ZnSO_4$ solution demonstrated that good quality QDs (photoluminescence quantum yield = 3.5%) were obtained when using NaHSe in short supply (by ca. 0.9-fold) relative to the mole amount of the Zn^{2+} precursor. A decrease (0.4 or 0.6) or an increase of the Zn/Se ratio (1.2 or 2.0) yielded ZnSe:Mn QDs with poor PL efficiency. It is well-known that Zn^{2+} precursors have a low reactivity towards NaHSe.[44] Increasing the concentration of $ZnSO_4$ (5.0 or 10.0 mM) while maintaining a Zn/Se molar ratio of 1/0.9 did not effectively improve the PL properties of ZnSe:Mn QDs (PL QY < 2%).

Influence of the pH. To improve the PL properties of the Mn-doped ZnSe QDs, that is, improvement of the Mn^{2+}-related $^4T_1 \rightarrow {}^6A_1$ emission and suppression of the trap emission, we also investigated the influence of the pH of the Zn^{2+}-MPA precursors solution using 4 % doping in Mn^{2+} and a Zn^{2+}/Se^{2-}/MPA molar ratio of 1/0.9/20. We found that when the pH of the Zn^{2+}/MPA precursors solution was set at 10.3 (the pH increased to 10.4 after the injection of the NaHSe solution), the as-prepared nanocrystals obtained after 24 h heating showed a strong orange emission at ca 595 nm and a very weak trap emission. When the pH value of the Zn^{2+}/MPA precursors was decreased below 10.0 (9.0 or 8.0), the

trap emission increased and the PL QY decreased (<1%). We fixed the pH value of the Zn^{2+}/MPA precursors solution at 10.3 in latter experiments.

Influence of the heating time. After the injection of NaHSe, small aliquots were removed from the reaction solution with a syringe to monitor the growth of nanocrystals via optical absorption. Using a Zn^{2+}/Se^{2-}/MPA molar ratio of 1/0.9/20 and 4% Mn^{2+} relative to Zn^{2+}, a well-resolved peak at 343 nm was observed after 15 min heating at 100°C indicating the homogeneous nucleation of small crystallites (Figure 1). The absorption peak attenuated sharply for longer growth times becoming a shoulder due to the Ostwald ripening process (formation of larger nanocrystals at the expense of smaller ones) and gradually red-shifted to 378 nm, which was consistent with the growth of the ZnSe host. The subtle blue-shift in absorption spectra observed after 24 h reflux (375 nm) may be a consequence of the partial decomposition of the MPA ligand surrounding the ZnSe:Mn core, leading to a sulfur-enriched shell.
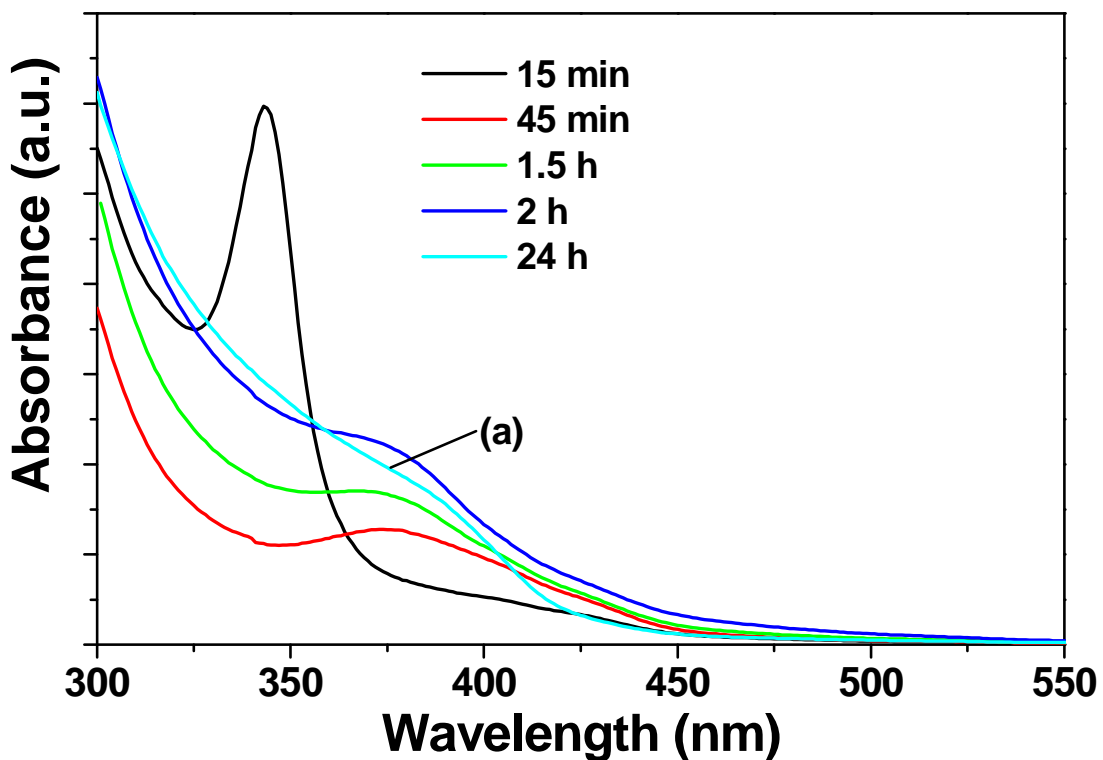

Figure 1. Temporal evolution of the UV-vis spectra of ZnSe:Mn@MPA nanocrystals grown at 100°C with a Zn^{2+}/Se^{2-}/MPA molar ratio of 1/0.9/20 and 4 % doping in Mn^{2+}.

The photoluminescence of the clear pale yellow solution was also monitored in the course of the nanocrystals growth. All aliquots taken during the first 5 h of growth exhibited at first no PL. Upon resting at room temperature, a strong orange-red emission evolved over a matter of hours (in some cases, minutes) (Figure 2). PL QYs measured from nanocrystals obtained after 30 min or 2 h of growth at 100°C and respectively 6 and 21 h storage at room temperature were high (23 and 19%, respectively, without any post-preparative treatment and the absence of the broad trap-emission centered at ca. 480 nm) (Figure 2). The photoluminescence decreased however gradually and disappeared after 24 h for the dots synthesized during 30 min at 100°C (Figure 2a). It should also be pointed out that the stability of the d-dots obtained after short heating times (< 3 h) was found to be modest. A deterioration of these nanocrystals accompanied by precipitation was generally observed after 48 h storage at room temperature. Good quality powder X-ray diffraction (XRD) patterns could also not be obtained for MPA-capped ZnSe:Mn QDs prepared during short reaction times (< 3 h). As the reaction prolonged, widths of the diffraction peaks were found to decrease and were more resolved (*vide infra*). The stability of ZnSe:Mn d-dots was markedly increased by extending the heating time at 100°C. No sign of macroscopic aggregation or loss of fluorescence were observed for the dots obtained after 24 h heating upon storage at room temperature for up to 3 months.

One interesting feature during the early stages of growth (15 min to 2 h) is the significant blue-shift of the maximum wavelength of the Mn^{2+} $^4T_1 \rightarrow {}^6A_1$ emission from 609 to 595 nm after excitation at 350 nm. Negatively-charged MPA ligands strongly interact with surface zinc atoms of small doped-ZnSe nanocrystals formed at the beginning of the growth stage. As a consequence, the d-orbitals of the Mn center will experience a high electric field difference along different directions, which results in a higher splitting of the energy levels.[29] Once the thickness of the ZnSe shell increases around the doped-ZnSe cores, the lattice field around Mn^{2+} ions becomes more symmetric leading to smaller splitting of the energy levels and a change of the PL color from orange-red to orange.
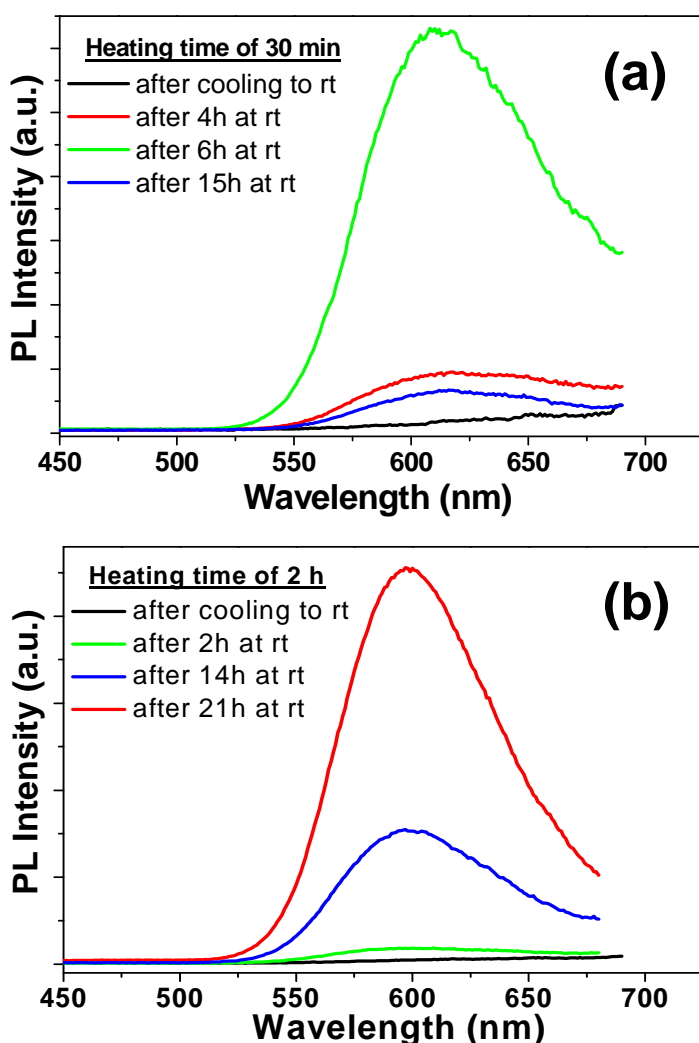
Figure 2. Temporal evolution of the PL spectra of ZnSe:Mn@MPA nanocrystals prepared with a Zn^{2+}/Se^{2-}/MPA molar ratio of 1/0.9/20 and 4 % doping in Mn^{2+} and grown at 100°C (a) during 30 min, (b) during 2 h. Excitation wavelength is 350 nm.

Influence of the ligand. We also tested the impact of various thiols (TGA, MHA, MSA and Cys) on the PL properties of ZnSe:Mn QDs when the Zn^{2+}/Se^{2-}/ligand molar ratio and the doping percentage were fixed at 1/0.9/20 and 4, respectively. All reactions were conducted at 100°C for 24 h. It was found that TGA-, MHA-, MSA-, and Cys-capped ZnSe:Mn QDs exhibited the Mn^{2+} $^4T_1 \rightarrow {}^6A_1$ transition at ca. 595 nm but the emissions were found to be broad (the full-width-at-half-maximum increased up to

10

94 nm while it was of ca. 60 nm for MPA-capped QDs). The PL QYs were also found to be weaker (< 1%) compared to nanocrystals prepared with MPA. The nanocrystal growth with TGA, MHA, MSA, and Cys ligands occurred finally with higher defect densities (increase of the ZnSe band-edge transition at ca. 460 nm). Compared to the other thiols used in this study, we suggest that MPA provides the better surface passivation of the QD crystalline lattice under our synthetic conditions.

Influence of the Mn^{2+} concentration. The ratio of Mn^{2+} relative to Zn^{2+} was varied from 1 to 6% to evaluate the effects of Mn^{2+} on the optical properties of the d-dots under the same experimental conditions (Zn^{2+}/NaHSe/MPA = 1/0.9/20, heating time of 24 h). While the dopant PL peak position and spectral contour were found to be independent of the Mn^{2+} concentration in the solution (PL emission at 596 nm and full-width-at-half-maximum of ca. 60 nm), an increase of the Mn^{2+} concentration from 1 to 4% relative to Zn^{2+} leads to an increase in the PL emission intensity, which also proves the successful incorporation of Mn^{2+} into ZnSe QDs (Figure 3). Further increasing the concentration of Mn^{2+} to 5 or 6% leads to a decrease of the PL QYs. The effect of Mn^{2+} ion concentration on the PL properties of Mn^{2+}-doped II-VI semiconductors QDs has been extensively studied in recent years and a so-called "concentration quenching effect" has been demonstrated.[45-48] When the concentration of Mn^{2+} becomes higher than a certain threshold, the non radiative energy transfers between neighboring Mn^{2+} dopant ions reduce and even annihilate the fluorescence. Under our synthetic conditions, the formation of such pairs of Mn^{2+} dopant ions is probably observed when the amount of Mn^{2+} ions in QDs is higher than 4 %. Energy Dispersive X-ray (EDX) spectroscopy experiments (*vide infra*) conducted on ZnSe:Mn@MPA QDs after purification indicated that the Mn^{2+} at. % was ca. 3%. This value is slightly higher than those used in organometallic syntheses (0.5-3% in growth solutions leading to nanocrystals doped with ca. 0.02-2.0 % Mn^{2+} ions).

It was also surprising to observe that the $^4T_1 \rightarrow {}^6A_1$ transition of Mn^{2+} ions is red-shifted by ca. 25 nm compared to the MPA-capped ZnSe:Mn QDs prepared by Wang *et al.*[41] using an aqueous route. As demonstrated by several groups,[49-51] the position Mn^{2+} emission peak is sensitive to the electric field imposed by the organic capping layer, to the Mn^{2+} radial positions, to the heating time, and to the Mn^{2+}

concentration inside the nanocrystals. Wang and coworkers used a theoretical concentration of Mn^{2+} twice lower than ours (4 versus 2) and heated the reaction mixture for 5 h, while the growth of our nanocrystals was performed during 24 h. A possible explanation for the red-shift observed with Mn-doped ZnSe dots prepared under our synthetic conditions is that the crystal field for each dopant ion became more symmetric in long range due to the thicker ZnSe shell formed. As a result, the crystal field splitting of Mn^{2+} d-orbitals became smaller, which resulted in a PL red-shift.
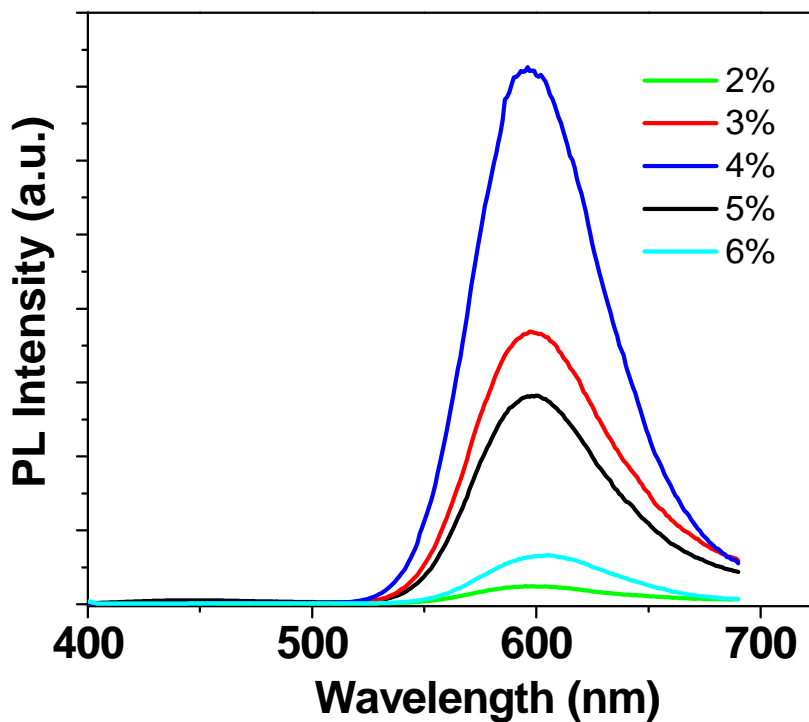
Figure 3. Influence of the concentration of Mn^{2+} relative to Zn^{2+} on PL spectra of ZnSe:Mn@MPA nanocrystals prepared with a $Zn^{2+}/Se^{2-}/MPA$ molar ratio of 1/0.9/20 and grown at 100°C for 24 h. Excitation wavelength is 350 nm.

3.2. Size, Shape, Crystal Structure and PL Properties of MPA-capped ZnSe:Mn d-dots. The dopants might also change the lattice structure of the ZnSe host material because the diameter of the Mn^{2+} ion (0.83 nm) is larger than that of the Zn^{2+} ion (0.74 nm).[52] To confirm that the crystal lattice of the ZnSe host nanocrystals was intact, powder XRD pattern of the MPA-capped ZnSe:Mn QDs was

recorded (Figure 4a). The XRD pattern of the nanocrystals exhibited characteristic peaks at ca. 27.5, 45.6, and 54.3° corresponding to the (111), (220) and (311) reflecting planes of cubic zinc blende ZnSe (JCPDS Card N° 80-0021). The peaks are broadened due to the finite crystalline size. These results prove that the ZnSe:Mn d-dots have a cubic zinc blende structure similar to undoped ZnSe QDs and confirm that the crystal lattice of the ZnSe host material is intact after doping with Mn^{2+} ions. A crystallite size of 3.5 ± 1.0 nm was estimated from the diffraction line broadening, value which correlated well with the results obtained from TEM analysis (vide infra). Finally, it is worth noting that the XRD patterns of the ZnSe:Mn QDs are located on higher angle compared to that of the pure ZnSe material probably because the MPA ligand partially decomposed by heating leading to a sulfur-enriched ZnS shell with smaller lattice parameters compared to ZnSe. The formation of alloyed doped-ZnSe(S) QDs is likely after 24 h heating at 100°C.
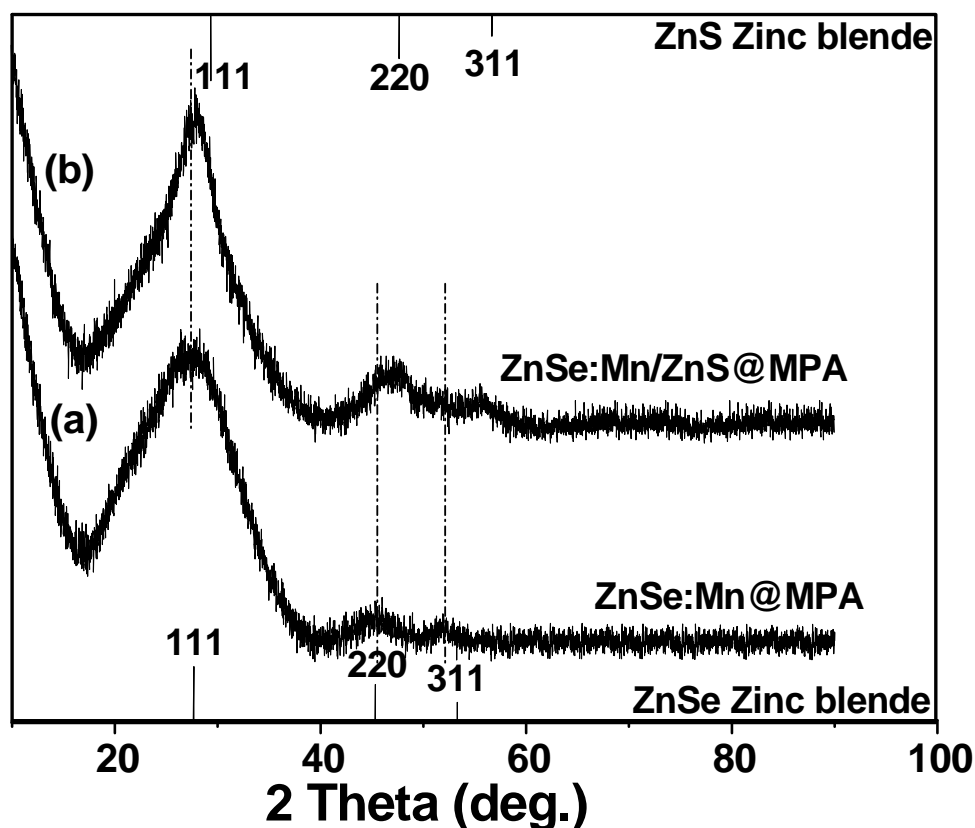

Figure 4. XRD patterns of ZnSe:Mn@MPA QDs (a) before and (b) after introduction of the ZnS shell.

Figure 5 presents UV-vis, PL, and PL excitation (PLE) spectra of ZnSe:Mn dots d-dots (~ 3 nm in size). The quantum confinement of an electron-hole pair caused a marked blue-shift in the absorption peak of ZnSe:Mn QDs obtained after 24 h heating at 100°C in comparison to the 442 nm (2.80 eV) band gap of the bulk ZnSe material. The nanocrystal R radius was calculated using the equation of quantum confinement written in the form:

$$E = Eg + \frac{\pi^2 \bar{h}^2}{2R^2} \left(\frac{1}{m_e} + \frac{1}{m_h} \right) - \frac{1.8e^2}{\varepsilon R}$$

where E is the energy of the first exited state, $Eg = 2.80$ eV is the band gap energy of bulk ZnSe, m_e and m_h are the effective masses of the electron and hole in ZnSe ($m_e = 0.15 m_o$, $m_h = 0.66\ m_o$, where $m_o = 9.11 \times 10^{-28}$ g is the free-electron mass), respectively, $\varepsilon = 9.2$ is the semiconductor dielectric constant, $\bar{h} = 6.58 \times 10^{-16}$ eV is the reduced Planck constant, and $e = 1.6 \times 10^{-9}$ C is the electron charge. Using the absorption peak for MPA-capped Mn-doped ZnSe QDs after 24 h of growth yields a nanocrystal diameter of 2.7 ± 0.4 nm. The deviation of 0.4 nm corresponds to ± 10 nm for the determination of the onset of absorption. The PLE spectrum corresponding to the 600 nm emission exhibits maximum at about 345 nm corresponding to the band gap excitation of host ZnSe nanocrystals.
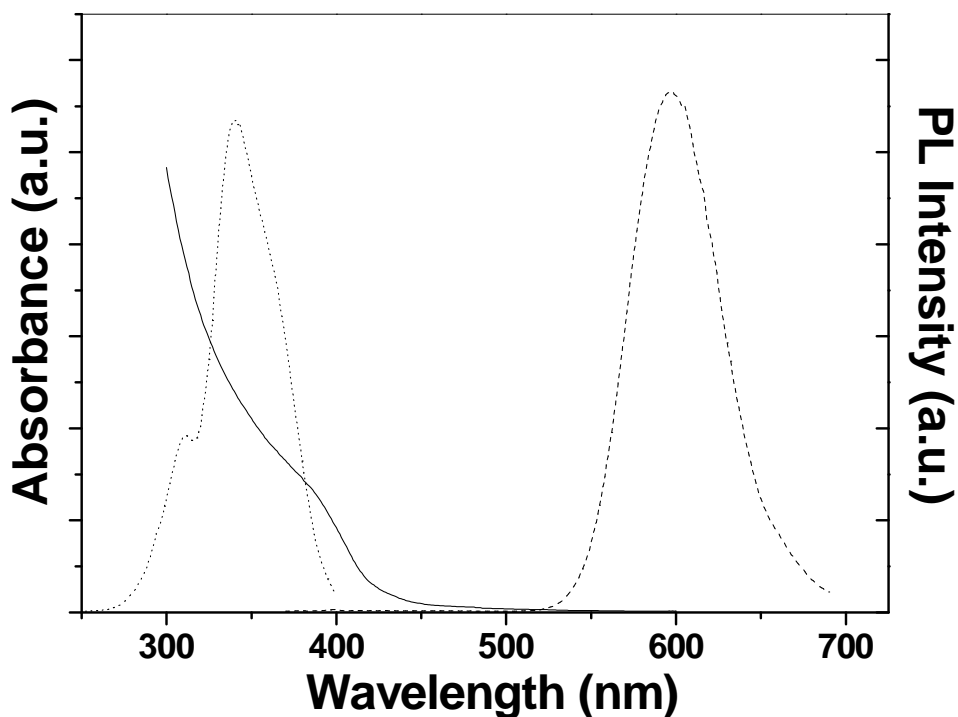
Figure 5. Optical absorption (solid line), PL excitation (doted line) and PL emission (dashed line) after excitation at 365 nm of MPA-capped ZnSe:Mn d-dots.

FT-IR spectra of the neutral MPA ligand and of the purified and dried ZnSe:Mn@MPA QDs are given in Figure 6. The acid function of MPA can clearly be identified on Figure 6a both through the very broad 3150 cm^{-1} O-H stretching vibration and through the 1718 cm^{-1} C=O stretching vibration. The strong vibration of the carbonyl group of MPA vanished upon surface functionalization of QDs. The symmetric and asymmetric stretching vibrations of the carboxylate group of the charged MPA appear at 1438 and 1575 cm^{-1}, respectively. The absence of SH stretch band between 2682-2561 cm^{-1} supports the attachment of the MPA ligand through covalent bonds between thiols and surface Zn atoms of ZnSe:Mn QDs. The spectrum of ZnSe:Mn QDs also displayed the bands assigned to the hydroxyl group of the acid function at 3432 cm^{-1} and of C-H stretching at 2921 cm^{-1}.
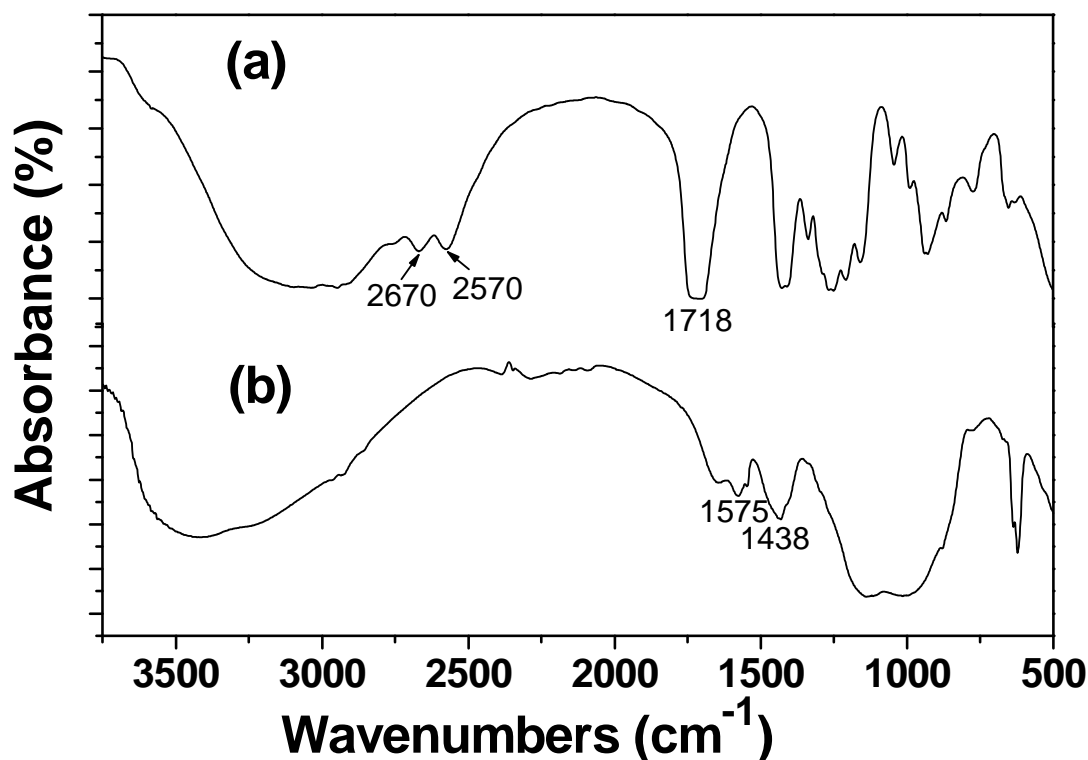
Figure 6. FT-IR spectra of (a) MPA and (b) ZnSe:Mn@MPA QDs.

Figure 7 shows a transmission electron microscopy (TEM) micrograph of 3.1 ± 0.3 nm diameter Mn-doped ZnSe QDs, corresponding to the final spectrum of Figure 1 with 3.5% PL QY (labelled a), which is in good accordance with the value calculated from the quantum confinement equation. Dynamic light-scattering (DLS) measurements indicate that the QDs are well-dispersed in water and that their hydrodynamic diameters range from 5 to 11 nm (average hydrodynamic diameter of 7.6 nm). The hydrodynamic diameter is larger than the diameter of the inorganic core due to the solvatation layer around the QDs in aqueous solution. Energy dispersive spectroscopy (EDS) measurements revealed that the atomic composition of the d-dots had a value similar to that of the ratios of precursors (see details in the core/shell subsection). An average diameter of 3.1 nm represents ca 88 ZnSe structural units in each

monocrystal (using a theoretical lattice parameter a of 0.56 nm, JCPDS Card N° 80-0021). Using 4% Mn^{2+} dopant means ca 14 Mn^{2+} ions per nanocrystal.
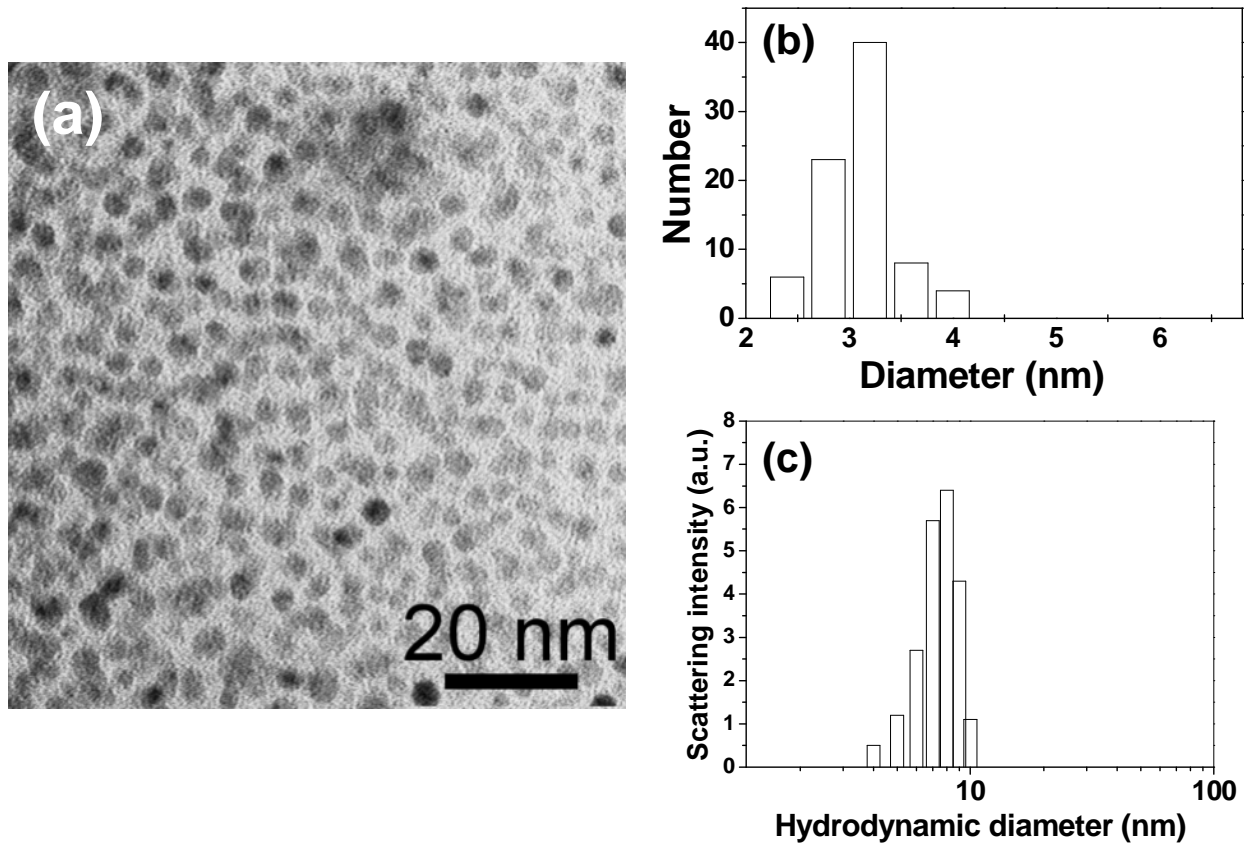

Figure 7. (a) TEM micrograph of ZnSe:Mn@MPA d-dots, (b) the corresponding particle size distribution, and (c) hydrodynamic size of ZnSe:Mn@MPA d-dots measured by DLS.

3.3. Epitaxial Growth of the ZnS Shell. A synthesis of core/shell ZnSe:Mn/ZnS QDs was also developed with the goal to improve the chemical, PL stabilities and QY of the QDs but also with the hope that the higher band gap ZnS shell with a small lattice mismatch with ZnSe (ca. 5%) will provide a diffusion barrier by stabilizing the Mn^{2+} doping ions. Although, there is no report on the preparation of ZnSe:Mn/ZnS d-dots, the preparation of ZnSe/ZnS d-dots in organic[31,53-56] or aqueous[57,58] solution has already been investigated by a few research groups. The ZnS shell was successfully introduced at the periphery of ZnSe:Mn cores by thermal decomposition at basic pH of Zn^{2+}/MPA complexes. The PL

intensity of Mn^{2+} that corresponds to the $^4T_1 \rightarrow {}^6A_1$ transition within the $3d^5$ configuration of Mn^{2+} increased gradually upon heating at 100°C and reached its maximum value (PL QY = 9%) after 10 h (Figure 8a). No improvement was observed by further heating. For ZnSe:Mn@MPA nanocrystals under the same heating conditions but in the absence of the Zn^{2+}/MPA complex, there is almost no change of PL QY. This suggests that the enhancement of PL QY is related to the growth of the ZnS shell. The enhanced QY of ZnS-capped ZnSe:Mn d-dots is a direct consequence of an effective surface passivation by which nonradiative recombination that compete with the regular luminescence are reduced significantly. A visual comparison of non-capped and of the ZnS-capped QDs is shown as inset in Figure 8b. Both samples are fluorescent under a handheld UV lamp providing 366 nm multiband irradiation, and it is obvious that the ZnS-passivated d-dots are much brighter. As shown in Figure 8b, the PL is shifted at 610 nm while it is located at 600 nm for the ZnSe:Mn core. Since Mn^{2+} had a higher affinity for ZnS than for ZnSe,[30] we suppose that surface Mn^{2+} ions of the ZnSe:Mn core diffuse into the ZnS lattice in which they are subjected to the electric field of the deprotonated MPA ligand. In the XRD pattern (Figure 4b), the peak positions shift to higher angles towards the position of ZnS, with peak widths and shapes being nearly unchanged, which proves the formation of core/shell ZnSe:Mn/ZnS QDs. This deviation could also result from the compression of the ZnS shell on the lattice planes of the doped-ZnSe core. Using TEM, the average diameter of core/shell nanocrystals obtained was found to be 4.3 ± 0.5 nm (average hydrodynamic diameter = 8.0 nm) (Figure 9). EDX measurements of the core ZnSe:Mn and of the core/shell ZnSe:Mn/ZnS QDs confirmed the nature of the materials (Figure 10). Zn, Se, and Mn peaks arise from the doped core while the detected S mainly comes from the capping MPA ligand. The presence of silica (peak at ca. 1.7 keV) may originate from a contamination of the samples by glassware during their storage. The growth of the ZnS shell around the ZnSe cores was clearly demonstrated by EDX experiments. With the deposition of the ZnS shell, the Zn/Se ratio increased from 1.02 in the ZnSe:Mn cores to 9.88 in the core/shell nanocrystals. In the meantime, the Zn/S atomic percentage decreased from 5.17 to 1.03.
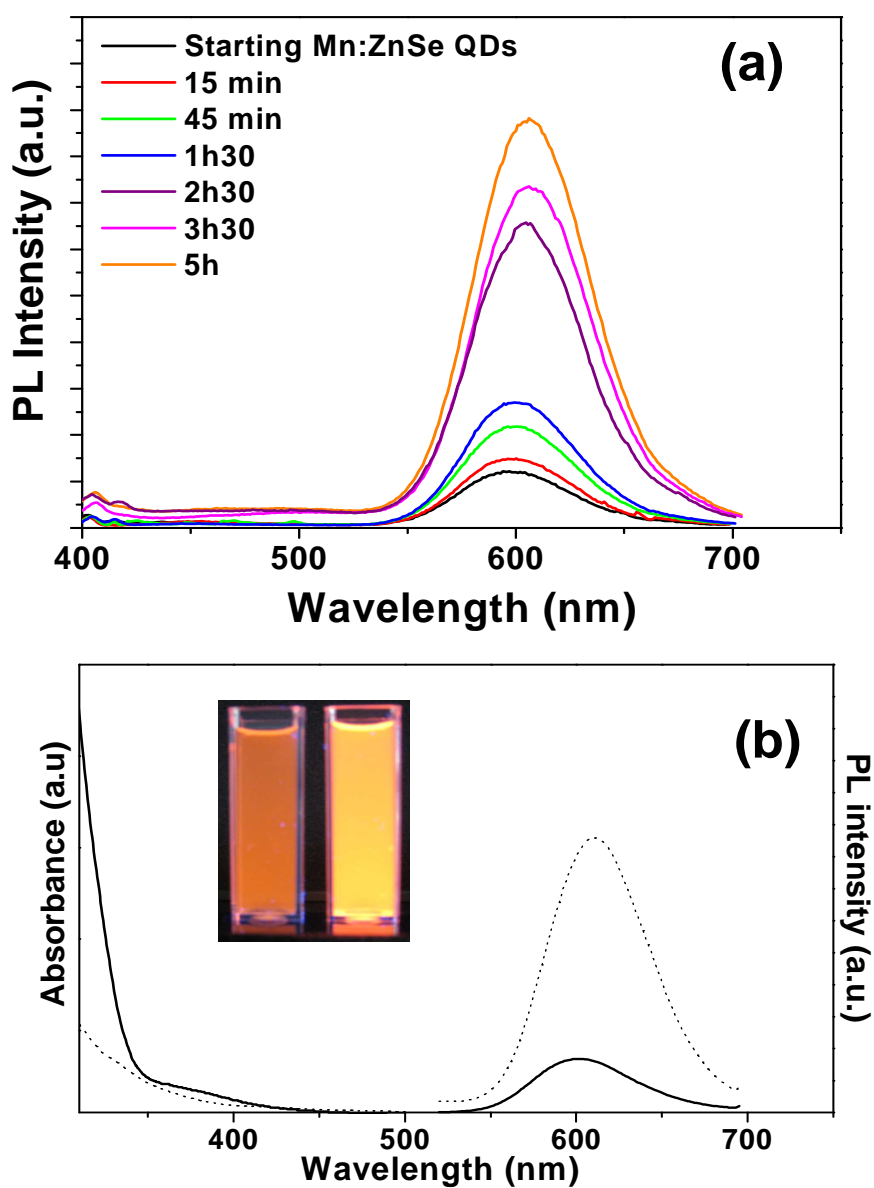
Figure 8. (a) Evolution of PL spectra during the overcoating of ZnSe:Mn QDs with the ZnS shell. (b) Absorption and PL spectra of ZnSe:Mn@MPA QDs before (solid) and after (dot) the introduction of the ZnS shell. Excitation wavelength is 350 nm. Inset shows digital pictures of the QDs before (left) and after (right) the overcoating with ZnS.
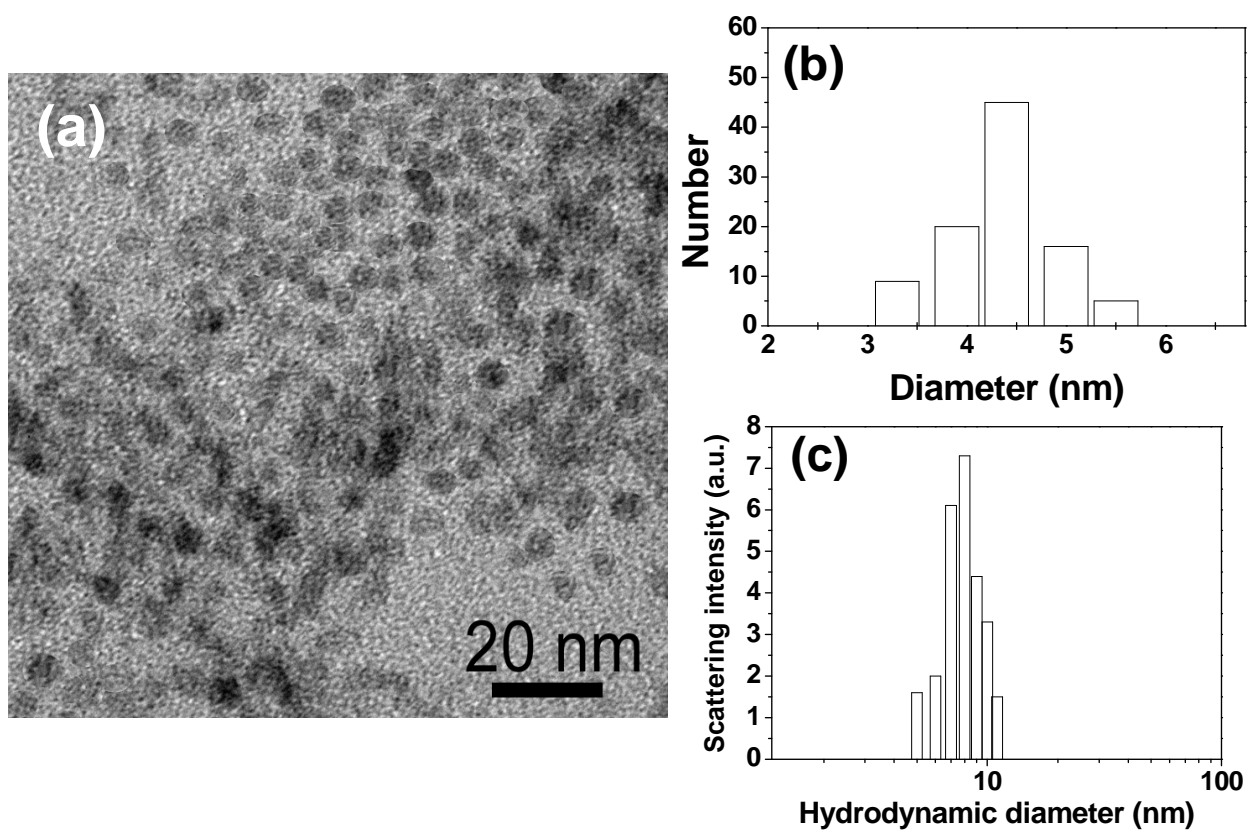
Figure 9. (a) TEM micrograph of core/shell ZnSe:Mn/ZnS@MPA d-dots, (b) the corresponding particle

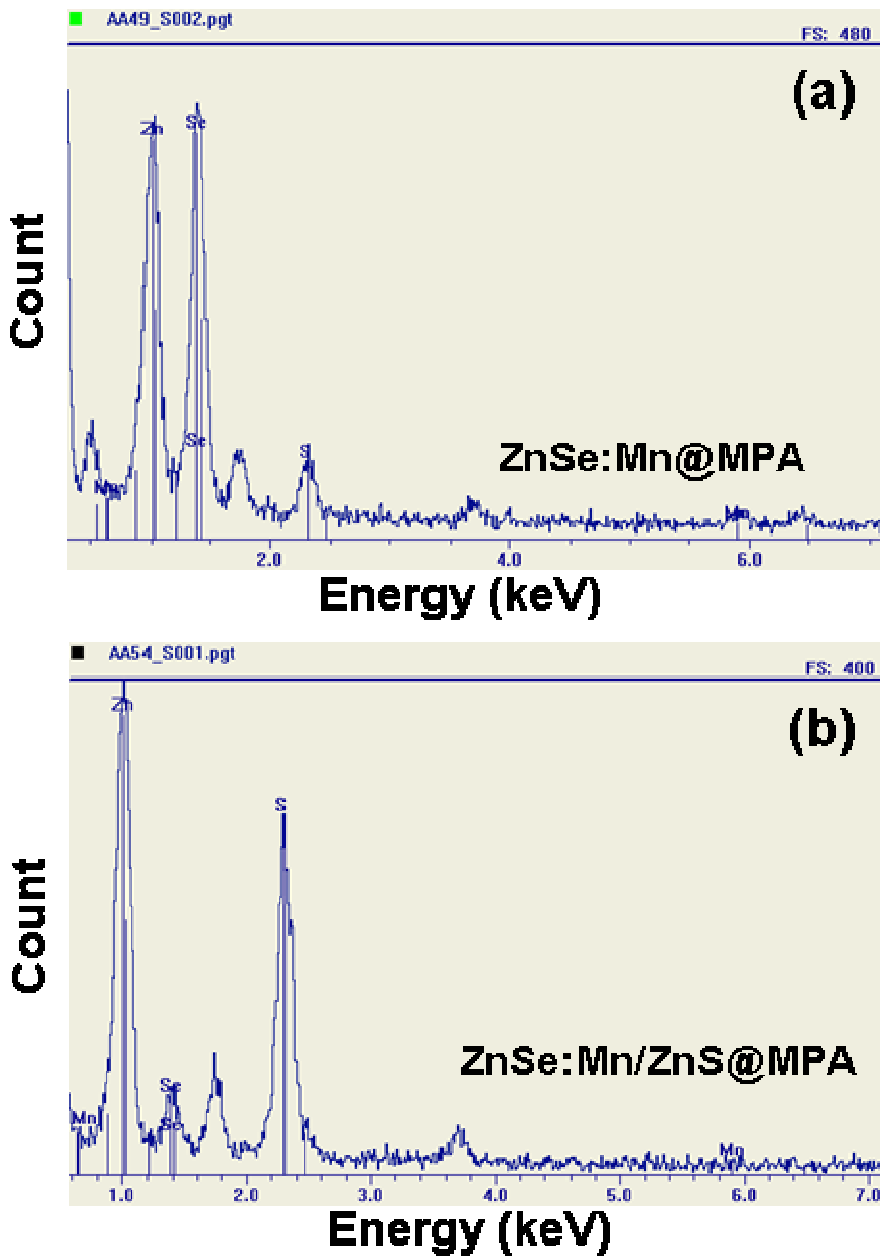size distribution, and (c) hydrodynamic size of ZnSe:Mn/ZnS@MPA d-dots measured by DLS.

Figure 10. EDX spectra of ZnSe:Mn@MPA QDs (a) before and (b) after the introduction of the ZnS shell.

The overcoating of ZnSe:Mn d-dots with ZnS was further confirmed by measuring the slow PL decay of the nanocrystals before and after surface modification. Indeed, Mn^{2+} ion emission lifetime is dependent on the diameter of the nanocrystals and is longer for QDs with thicker overcoating layer or thicker diffusion region.[59] The slow PL decay curves of Mn^{2+} ions for the core ZnSe:Mn and the

core/shell ZnSe:Mn/ZnS QDs are shown in Figure 11. The slow decay times, attributed to the emission of the single isolated Mn^{2+} ions in a cubic site,[60-62] were 0.62 and 1.39 ms for the core and core/shell QDs, respectively. Interestingly, the shell dependence of the PL lifetime is related to the PL QY. After introduction of the shell, the PL QY increased by 257% (from 3.5 to 9%) while the PL lifetime was found to increase by 224%.
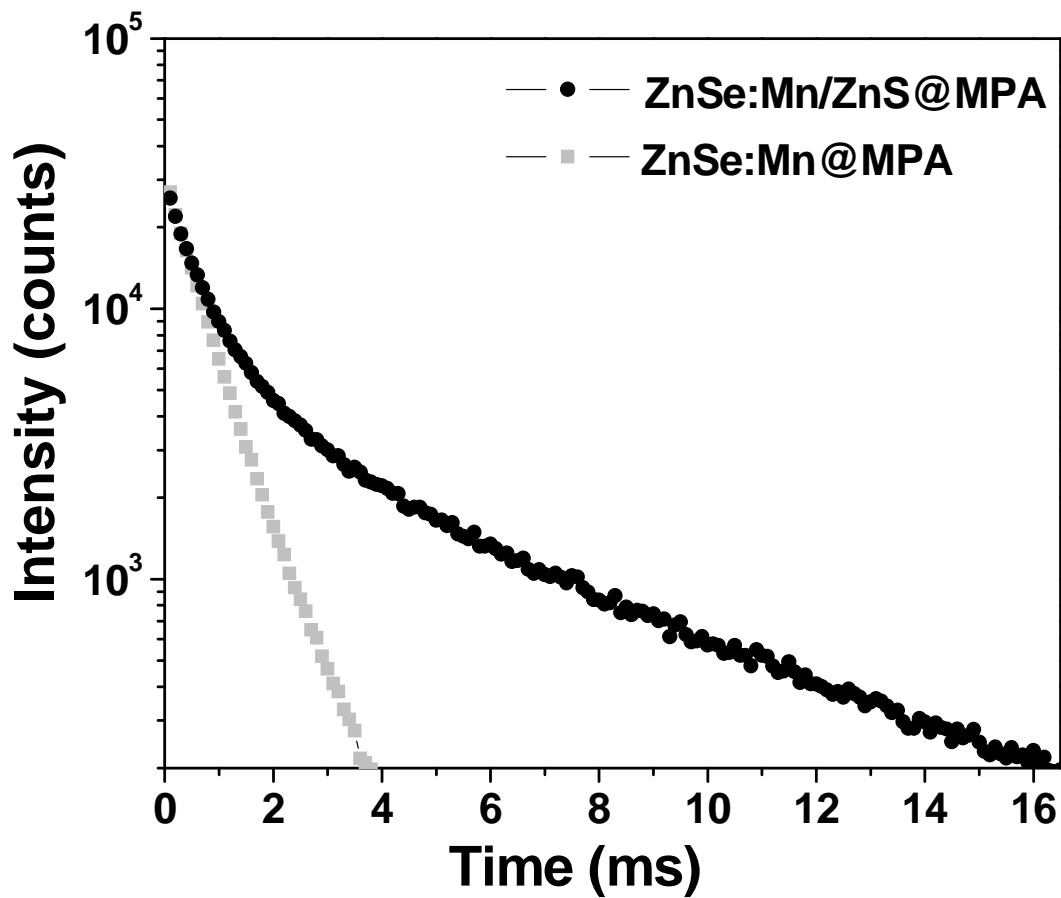

Figure 11. PL decay curves recorded at room temperature of ZnSe:Mn and ZnSe:Mn/ZnS QDs at a wavelength near 605 nm.

3.4. Effects of pH on MPA-capped ZnSe:Mn/ZnS QDs PL. For the efficient and reliable utilization of semiconductor nanocrystal technology especially in biological applications, it is important to evaluate the external factors that may affect the optical properties of the QDs. As shown in Figure 12, MPA-

capped ZnSe:Mn/ZnS QDs are sensitive to pH with greater fluorescence at higher pH (PL QY = 12.5% at pH = 12). The PL QY at neutral pH is 8.9 %. A rapid decay of PL was observed when the pH was below 6.0 (PL QY = 2.5% at pH = 4). Under pH = 4.0, the QDs became unstable in the acidic aqueous environment, they precipitated and the PL disappeared.
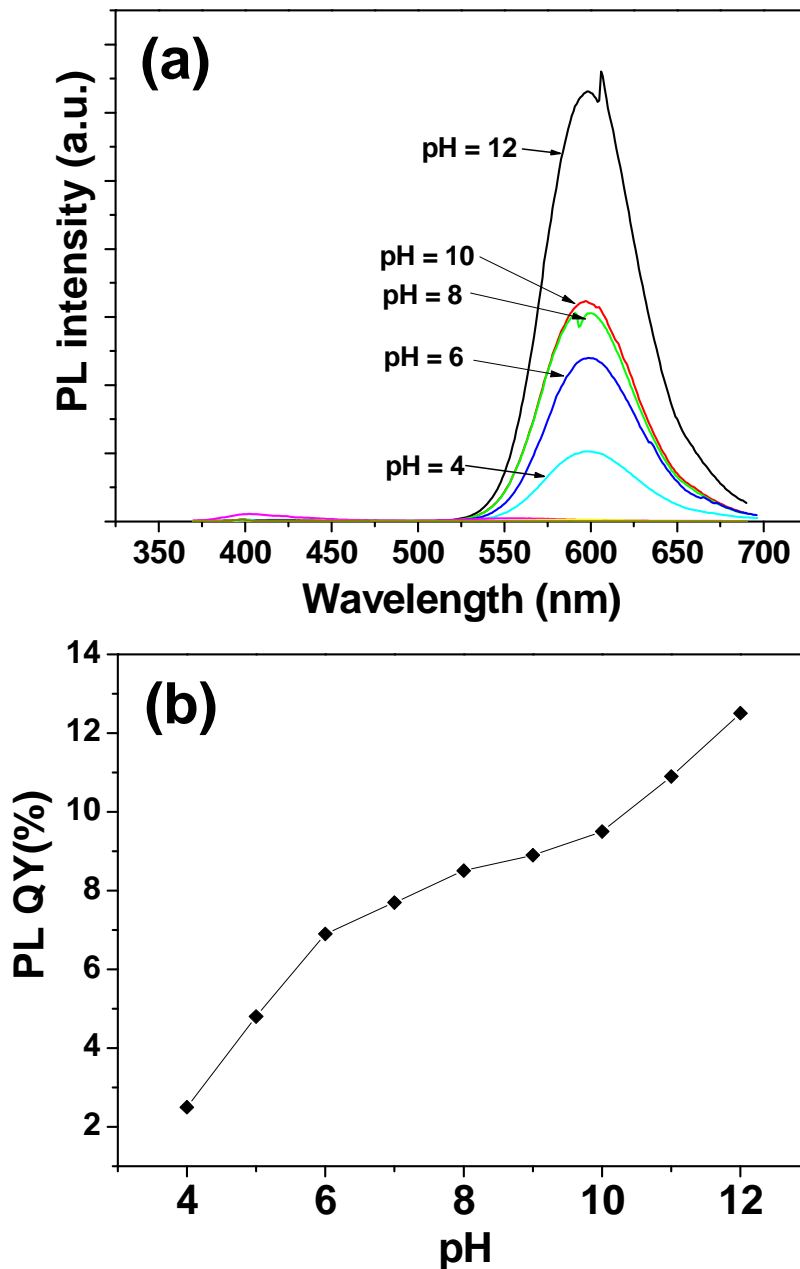

Figure 12. (a) Fluorescence spectra of ZnSe:Mn/ZnS QDs in aqueous solution at different pH values. (b) Effect of pH on the PL QY of ZnSe:Mn/ZnS@MPA QDs.

4. Conclusions

We have developed a new synthetic method to prepare in aqueous solution highly luminescent and monodisperse Mn-doped ZnSe d-dots and demonstrated that molar ratios of precursors, Mn^{2+} concentration, pH value, heating time and stabilizer play an important role in determining the stability and optical properties of these nanoparticles. Among the tested stabilizer, 3-mercaptopropionic acid is superior in terms of high PL QY and low trapping emission. The PL properties were markedly improved by overcoating the Mn-doped ZnSe core with a ZnS shell. The core/shell ZnSe:Mn/ZnS QDs had a PL QY of ca. 9% in water at neutral pH, a good crystallinity and a diameter of ca. 4.3 nm. It is hoped that ZnSe:Mn/ZnS core/shell QDs prepared by this convenient procedure will find diverse biological applications in areas where water-soluble QDs with high PL efficiency and long-term stability are needed.

References

(1)   Bruchez, Jr, M.; Moronne, M.; Gin, P.; Weiss, S.; Alivisatos, A. P. *Science* **1998**, *281*, 2013.

(2)   Chan, W.C.W.; Nie, S. *Science* **1998**, *281*, 2016.

(3)   Han, M.; Gao, X.; Su, J.Z.; Nie, S. *Nat. Biotechnol*. **2001**, *19*, 631.

(4)   Medintz, I. L.; Uyeda, H. T.; Goldman, E. R. Mattoussi, H. *Nat. Mater*. **2005**, *4*, 435.

(5)   Weng, J.; Ren, J. *Curr. Med. Chem*. **2006**, *13*, 897.

(6)   Sun, Q. J.; Wang, Y. A.; Li, L. S.; Wang, D. Y.; Zhu, T.; Xu, J.; Yang, C. H.; Li, Y. F. *Nat. Photonics* **2007**, *1*, 717.

(7)   Jamieson, T.; Bakhshi, R.; Petrova, D.; Pocock, R.; Imani, M. *Biomaterials* **2007**, *28*, 4717.

(8)   Romero, M. J.; van de Lagemaat, J.; Mora-Sero, I.; Rumbles, G.; Al-Jassim, M. M. *Nano Lett.* **2006**, *6*, 2833.

(9)   Yong, K. -T.; Roy, I.; Pudavar, H. E.; Bergey, E. J.; Tramposch, K. M.; Swihart, M. T.; Prasad, P. N. *Adv. Mater.* **2008**, *20*, 1412.

(10)   Michalet, X.; Pinaud, F. F.; Bentolila, L.A.; Tsay, J. M.; Doose, S.; Li, J. J.; Sundaresan, G.; Wu, A. M.; Gambhir, S. S. Weiss S. *Science* **2005**, *307*, 538.

(11)   Hild, W. A.; Breunig, M.; Goepferich, A. *Eur. J. Pharm. Biopharm.* **2008**, *68*, 153.

(12)   Xu, G.; Yong, K. -T.; Roy, I.; Mahajan, S. D.; Ding, H.; Schwartz, S. A.; Prasad, P. N. *Bioconjugate Chem.* **2008**, *19*, 1179.

(13)   Norris, D. J.; Efros, A. L.; Erwin, S. C. *Science* **2008**, *319*, 1776.

(14)   Hu, H.; Zhang, W. *Opt. Mater.* **2006**, *28*, 536.

(15)   Kim, C.C.; Sivananthan, S. *Phys. Rev. B* **1996**, *53*, 1475.

(16)   Yu, H.; Li, J.; Loomis, R. A.; Gibbons, P. C.; Wang, L. W.; Buhro, W. E. *J. Am. Chem. Soc.* **2003**, *125*, 16168.

(17)   Jun, Y. W.; Koo, J. E.; Cheon, J. *Chem. Commun.* **2000**, 1243.

(18)   Heulings, H. R.; Huang, X. Y.; Li, J. *Nano Lett.* **2001**, *1*, 521.

(19)   Kennedy, T. A.; Glaser, E. R.; Klein, P. B.; Bhargava, R. N. *Phys. Rev. B* **1995**, *52*, R14356.

(20)   Hines, M. A.; Guyot-Sionnest, P. *J. Phys. Chem. B* **1998**, *102*, 3655.

(21) Reiss, P.; Quemard, G.; Carayon, S.; Bleuse, J.; Chaudezon, F.; Pron, A. *Mater. Chem. Phys.* **2004**, *84*, 10.

(22) Chen, H. -S.; Lo, B.; Hwang, J. -Y.; Chang, G. Y.; Chen, C. -M.; Tasi, S. -J.; Jassy Wang, S. -J. *J. Phys. Chem.* B **2004**, *108*, 17119.

(23) Reiss, P. *New. J. Chem.* **2007**, *31*, 1843.

(24) Nemchinov, A.; Kirsanova, M.; Hewa-Kasakarage, N.N.; Zamkov, M. *J. Phys. Chem. C* **2008**, *112*, 9301.

(25) Choy, W. C. H.; Xiong, S.; Sun, Y. *J. Phys. Chem. D: Appl. Phys.* **2009**, *42*, 125410.

(26) Pradan, N.; Goorskey, D.; Thessing, J.; Peng, X. *J. Am. Chem. Soc.* **2005**, *127*, 17586.

(27) Zu, L.; Norris, D. J.; Kennedy, T. A.; Erwin, S. C.; Efros, A. L. *Nano Lett.* **2006**, *6*, 334.

(28) Pradhan, N.; Battaglia, D. M.; Liu, Y.; Peng, X. *Nano Lett.* **2007**, *7*, 312.

(29) Pradhan, N.; Peng, X. *J. Am. Chem. Soc.* **2007**, *129*, 3339.

(30) Thakar, R.; Chen, Y.; Snee, P. T. *Nano Lett.* **2007**, *7*, 3429.

(31) Shen, H.; Wang, H.; Li, X.; Niu, J. Z.; Wang, H.; Chen, X.; Li, L. S. *Dalton Trans* **2009**, 10534.

(32) Zeng, R.; Rutherford, M.; Xie, R.; Zou, B.; Peng, X. *Chem. Mater.* **2010**, *22*, 2107.

(33) Acharya, S.; Sarma, D. D.; Jana, N. R.; Pradhan, N. *J. Phys. Chem. Lett.* **2010**, *1*, 485.

(34) Lan, G. -Y.; Lin, Y. -W.; Huang, Y. -F.; Chang, H. -T. *J. Mater. Chem.* **2007**, *17*, 2661.

(35) Zheng, Y.; Yang, Z.; Ying, J. Y. *Adv. Mater.* **2007**, *19*, 1475.

(36) Andrade, J. J.; Brasil Jr, A. G.; Farias, P. M. A.; Fontes, A.; Santos, B. S. *Microelectronics J.* **2009**, *40*, 641.

(37) Gong, H.; Lin, Z.; Zhai, G.; Liu, K.; Wang, Z.; Huo, X.; Li, J.; Huang, H.; Wang, M. *Ceramics Int*. **2008**, *34*, 1085.

(38) Deng, Z.; Lie, F. L.; Shen, S.; Ghosh, I.; Mansuripur, M.; Muscat, A. J. *Langmuir* **2009**, *25*, 434.

(39) Fang, Z.; Li, Y.; Zhang, H.; Zhong, X.; Zhu, L. *J. Phys. Chem. C* **2009**, *113*, 14145.

(40) Qian, H.; Qiu, X.; Li, L.; Ran, J. *J. Phys. Chem. B* **2006**, *110*, 9034.

(41) Wang, C.; Gao, X.; Ma, Q.; Su, X. *J. Mater. Chem*. **2009**, *19*, 7016.

(42) Klayman, D. L.; Griffin, T. S. *J. Am. Chem. Soc*. **1973**, *95*, 197.

(43) Fischer, M.; Georges, J. *Chem. Phys. Lett*. **1996**, *260*, 115.

(44) Ge, J. P.; Xu, S.; Zhuang, J.; Wang, X.; Peng, Q.; Li, Y. D. *Inorg. Chem*. **2006**, *128*, 4922.

(45) de Visschere, P.; Neyts, K. *J. Lumin*. **1992**, *52*, 313.

(46) Vyas, P. D.; Kulkarni, S. K. *Appl. Phys. Lett*. **1995**, *67*, 2506.

(47) Sooklal, K.; Cullum, B .S.; Angel, S. M.; Murphy, C. J. *J. Phys. Chem*. **1996**, *10*0, 4551.

(48) Peng, W. Q.; Qu, S. C.; Cong, G. W.; Wang, Z. G. *J. Crystal Growth* **2005**, *279*, 454.

(49) Barthou, C.; Benoit, J.; Bennaloul, P.; Morell, A. *J. Electrochem. Soc*. **1994**, *141*, 524.

(50) Ronda, C.R.; Amrein, T. *J. Lumin*. **1996**, *69*, 245.

(51) Bol, A.A. ; Meijerink, A. *J. Phys. Chem. B* **2001**, *105*, 10197.

(52) Shannon, R. D. *Acta Crystallogr., Section A* **1976**, 32, 751.

(53) Song, K. -K.; Lee, S. *Curr. Appl. Phys*. **2001**, *1*, 169.

(54) Hwang, C. -S.; Cho, I. -H. *Bull. Korean Chem. Soc*. **2005**, *26*, 1776.

(55) Ali, M.; Sarma, D. D. *J. Nanosci. Nanotech.* **2007**, *7*, 1960.

(56) Lad, A. D.; Mahamuni, S. *Phys. Rev. B* **2008**, *78*, 125421.

(57) Wing, G.; Ji, W.; Zheng, Y.; Ying, J. Y. *Optics Express* **2008**, *16*, 5710.

(58) Matylitsky, V. V.; Shavel, A.; Gaponik, N.; Eychmüller, A.; Wachtveitl, J. *J. Phys. Chem. C* **2008**, *112*, 2703.

(59) Gan, C.; Zhang, Y.; Battaglia, D.; Peng, X.; Xiao, M. *Appl. Phys. Lett*. **2008**, *92*, 241111.

(60) Bol, A. A.; Meijerink, A. *Phys. Rev. B* **1998**, *58*, R15997.

(61) Smith, B. A.; Zhang, J. Z.; Joly, A.; Liu, J. *Phys. Rev. B* **2000**, *62*, 2021.

(62) Zheng, J.; Yuan, X.; Ikezawa, M.; Jing, P.; Liu, X.; Zheng, Z.; Kong, X.; Zhao, J.; Masumoto, Y. *J. Phys. Chem. C* **2009**, *113*, 16969.

SYNOPSIS TOC (Word Style "SN_Synopsis_TOC").
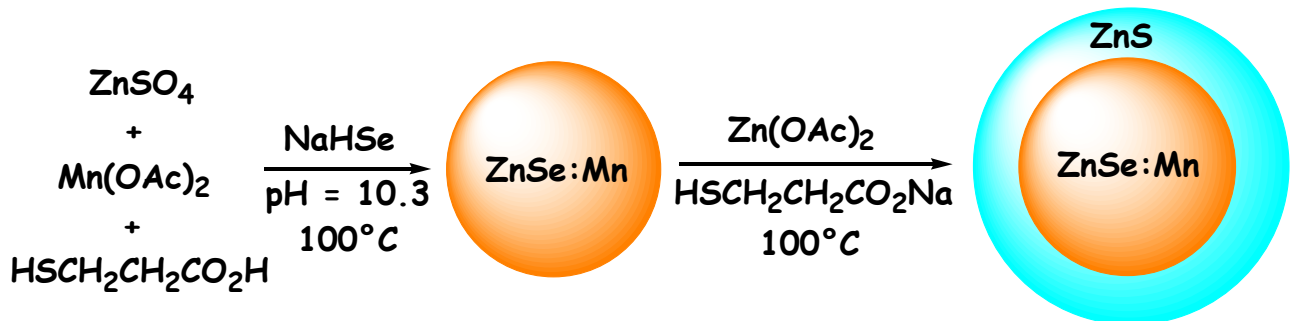
Highly luminescent manganese-doped zinc selenide (ZnSe:Mn) quantum dots were synthesized in aqueous solution at 100°C using the nucleation-doping strategy. The influence of various experimental variables, including Mn^{2+} concentration, $Zn^{2+}/Se^{2-}/3$-mercaptopropionic acid molar ratio, and reaction time have been systematically investigated to obtain quantum dots with high optical quality and pure dopant emission. Overcoating a high bandgap ZnS shell around the ZnSe:Mn cores allows significant improvement of the photoluminescence properties of the nanocrystals. A 2.5-fold increase in photoluminescence quantum yield (from 3.5 to 9%) and of Mn^{2+} ion emission lifetime have been observed after surface passivation.